

# High-precision SIMS oxygen, sulfur and iron stable isotope analyses of geological materials: accuracy, surface topography and crystal orientation

N. T. Kita,\* J. M. Huberty, R. Kozdon, B. L. Beard and J. W. Valley

A high-precision SIMS analysis technique has been established for oxygen, sulfur, and iron isotope ratios and applied to a wide range of geoscience research areas using a Cameca IMS-1280 at the Wisconsin Secondary Ion Mass Spectrometer Laboratory (WiscSIMS). Precision and accuracy of 0.3‰ is achieved routinely for the measurement of  $^{18}\text{O}/^{16}\text{O}$  ratio using multicollection Faraday Cup (FC) detectors and primary  $\text{Cs}^+$  beam size of 10  $\mu\text{m}$ . Smaller beam sizes of 3  $\mu\text{m}$  to <1  $\mu\text{m}$  yield precisions of 0.7–2‰ using a multicollection Electron Multiplier (EM) in pulse-counting mode for  $^{18}\text{O}$ . We evaluate small SIMS analytical biases at the level of a few ‰ or less using standard minerals with homogeneous oxygen isotope ratios: (i) topography of samples related to polishing relief of grains and location of analysis in a sample holder; and (ii) crystal orientation effects in magnetite ( $\text{Fe}_3\text{O}_4$ ). The latter effect has not been detected for oxygen isotope ratio measurements in other minerals including a variety of silicate, oxide, and carbonate minerals at WiscSIMS. However, similar analytical biases that are correlated with crystal orientation have been identified from Fe isotope analyses in magnetite and S isotope analysis in sphalerite (ZnS), and many minerals have not yet been evaluated. The total range of analytical bias among randomly oriented magnetite grains becomes smaller by reducing the sputtering energy of the primary ions (from 20 to 10 keV), which may help reduce crystal orientation effects. Copyright © 2010 John Wiley & Sons, Ltd.

**Keywords:** Secondary Ion Mass spectrometer; geology; isotope ratio; crystal orientation; magnetite

## Introduction

High precision and accuracy for oxygen isotope analyses of geological samples are important for understanding a wide range of geologic processes and materials.<sup>[1]</sup> Important geologic records are often found from micron-scale objects showing less than a few ‰ (permil = 0.1%) variations in their  $^{18}\text{O}/^{16}\text{O}$  ratios, such as zoned zircon crystals, speleothems, and carbonate shells of foraminifera.<sup>[1–3]</sup> At WiscSIMS, we have established high-precision ( $\leq 0.3\%$ ) oxygen isotope measurements from 10  $\mu\text{m}$  analysis spots using a Cameca IMS-1280, the latest large radius magnetic sector SIMS equipped with a multicollection system that includes a total of 10 ion detectors.<sup>[4]</sup> A stable and efficient isotopic analysis is enabled with the IMS-1280 compared to earlier IMS-1270 instruments due to hardware and software improvements, such as magnetic field regulation using nuclear magnetic resonance (NMR, stability better than 10 ppm in mass over 10 h) and automatic recentering of secondary ions in the field aperture at each analysis spot.

In this report, we summarize the high-precision oxygen isotope analysis technique employed at WiscSIMS, and address the reproducibility of analyses. Further, we evaluate various instrumental biases due to sample matrix, topography, and crystal orientation. Recent geological and environmental applications using an IMS-1280 are reviewed elsewhere.<sup>[1]</sup>

## Typical Analytical Conditions of IMS-1280

For oxygen two-isotope ( $^{18}\text{O}/^{16}\text{O}$ ) analyses,  $\text{Cs}^+$  primary ions (+10 kV) are focused to beam sizes of 10  $\mu\text{m}$  diameter at the

intensity of 2.5 nA, and secondary ions are accelerated as negative  $\text{O}^-$  ions (–10 kV). Two isotopes of oxygen,  $^{16}\text{O}^-$  and  $^{18}\text{O}^-$ , are detected by FC detectors simultaneously at intensities of  $3 \times 10^9$  and  $6 \times 10^6$  cps, respectively. The electron gun (–10 kV) is used for charge compensation because most geological samples are either insulators and/or mounted in epoxy resin, which are Au or C coated. In order to maximize secondary ion transmission at the given mass resolving power (in this case,  $\sim 2200$  at 10% peak height), transfer lens optics are tuned at magnifications of 200. The contrast aperture, entrance slit, field aperture, and energy slit are set to 400  $\mu\text{m}$  diameter, 120  $\mu\text{m}$  width,  $4000 \times 4000 \mu\text{m}$  square, and 40 eV width at low-energy peak, respectively. The transmission of the secondary ions is  $\sim 90\%$  compared to the condition where all secondary apertures and slits are fully opened. The useful yield of oxygen from silicate minerals is estimated to be about 7%.<sup>[4]</sup>

A single analysis takes 3 minutes including time for presputtering (10 s), automatic centering of secondary ions ( $\sim 60$  s, scan of the first deflector in the secondary optics against the field aperture, DTFA-XY), and integration of the oxygen isotope signal (total 80 s: 4 s  $\times$  20 cycles). The spot-to-spot reproducibility of  $^{18}\text{O}/^{16}\text{O}$  ratios in repeated analyses of homogeneous isotope standards is

\* Correspondence to: N. T. Kita, WiscSIMS and NASA Astrobiology Institute, Department of Geoscience, University of Wisconsin-Madison, 1215 W. Dayton St., Madison, WI 53706, USA. E-mail: noriko@geology.wisc.edu

WiscSIMS and NASA Astrobiology Institute, Department of Geoscience, University of Wisconsin-Madison, 1215 W. Dayton St., Madison, WI 53706, USA

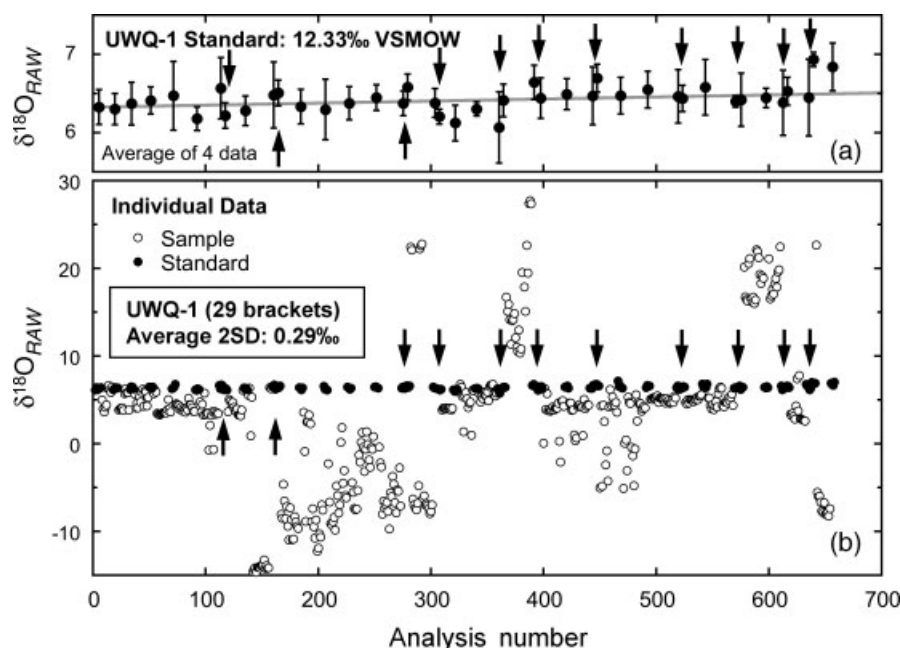


**Figure 1.** Reproducibility of SIMS  $\delta^{18}\text{O}_{\text{RAW}}$  values of quartz standard UWQ-1 ( $\delta^{18}\text{O} = 12.33\text{‰}$  SMOW) during one 48-h session.<sup>[4]</sup> The 658 spot analyses include 173 on standards. Four spots on UWQ-1 standard were analyzed (filled circles) between every 10–20 unknown samples (open circles). The average and 2SD of  $\delta^{18}\text{O}_{\text{RAW}}$  values of 8 standards that bracket a set of unknown analyses are used to calculate instrumental bias and external reproducibility, respectively. The average value of 2SD from 29 sets of bracket standard analyses is 0.29‰ during this session. (a) The average of each group of four standard analyses. Arrows indicate sample changes. (b) Individual data.

typically  $\pm 0.3\text{‰}$  (2SD, standard deviation), which is similar to the internal precision of 20 cycles (0.2‰ in 2SE, standard error of the mean) due to thermal drift of FC detector at the level of 1000 cps (using  $10^{11} \Omega$  amplifier for  $^{18}\text{O}$ ). Since the long-term drift of the FC detector is less than 1000 cps, FC baseline is measured only once at the beginning of a 12-h session. A series of 10–20 unknown analyses are bracketed by a set of 8 analyses of a standard grain mounted at the center of the same epoxy disk, which are used to evaluate the instrumental bias and external reproducibility. In two days of one continuous session (48 h), more than 650 spot analyses were made that include 173 standard analyses and multiple sample changes (Fig. 1). Usually, there is no significant drift of standard data through a session or between sample changes.

For convenience, the measured ( $^{18}\text{O}/^{16}\text{O}$ ) ratios are converted to  $\delta$  notation as permil deviation from Standard Mean Ocean Water (SMOW).

$$\delta^{18}\text{O}_{\text{RAW}} = \left[ \frac{(^{18}\text{O}/^{16}\text{O})_{\text{RAW}}}{(^{18}\text{O}/^{16}\text{O})_{\text{SMOW}}} - 1 \right] \times 1000(\text{‰}) \quad (1)$$

where  $(^{18}\text{O}/^{16}\text{O})_{\text{SMOW}} = 0.00200520$ <sup>[5]</sup> and suffix *RAW* indicates the value obtained from the SIMS. Instrumental bias is obtained by comparison of  $\delta^{18}\text{O}_{\text{RAW}}$  and  $\delta^{18}\text{O}$  on the SMOW scale, which can be determined from laser fluorination and gas-source mass spectrometry.<sup>[6]</sup> The bias at WiscSIMS varies among silicate and oxide minerals from  $-5\text{‰}$  in quartz ( $\text{SiO}_2$ ) and  $+11\text{‰}$  in titanite ( $\text{CaTiSiO}_5$ ), showing strong matrix effects as summarized in Valley and Kita.<sup>[1]</sup>

The smallest primary Cs-beam size achievable by IMS-1280 is  $\sim 0.3 \mu\text{m}$ , however, primary and secondary ion intensities become too low to obtain high-precision oxygen isotope ratios. Our practical minimum beam size is  $0.5 \times 0.9 \mu\text{m}$  at primary  $\text{Cs}^+$  intensity of 1–2 pA,<sup>[7]</sup> though a beam size of  $\sim 2 \mu\text{m}$  at 20–30 pA is

more practical for isotopic analysis.<sup>[3,8]</sup> For primary beam intensity  $> 1 \text{ pA}$ , the intensity of secondary  $^{16}\text{O}$  ions is above  $10^6$  cps and measured by FC detector in order to avoid QSA (quasi simultaneous arrival) effects.<sup>[9]</sup> For a primary beam intensity of 1–30 pA, the  $^{18}\text{O}$  signal is typically in the range of  $2 \times 10^3 - 5 \times 10^4$  cps and measured using an EM detector. A single analysis takes 15–30 min, depending on the secondary  $^{18}\text{O}$  intensity in order to accumulate enough counts to obtain good counting statistics. The external precision of ( $^{18}\text{O}/^{16}\text{O}$ ) ratios is typically 0.7‰ (2SD) for  $2 \mu\text{m}$  spots, and  $\sim 2\text{‰}$  (2SD) for  $\leq 1 \mu\text{m}$  spots.<sup>[3,7]</sup>

## Effect of Topography

Kita *et al.*<sup>[4]</sup> extensively examined the effect of surface topography on the measured oxygen isotope ratio using an IMS-1280. Many geological samples are mounted in epoxy resin, and difference in hardness among minerals and epoxy often creates significant polishing relief. Kita *et al.*<sup>[4]</sup> show a correlation between the amount of polishing relief and the reproducibility of oxygen isotope analyses by using zircon standard grains ( $\text{ZrSiO}_4$ ) with homogeneous oxygen isotope ratios. As shown in Fig. 2, the SIMS  $\delta^{18}\text{O}_{\text{RAW}}$  values are poorly reproduced with 2SD of 2.5‰ when the standard grain shows a significant polishing relief of  $\sim 20 \mu\text{m}$ . This effect is even worse if sample surfaces are not normal to the axis of the secondary beam. By grinding and repolishing samples to reduce the polishing relief (diamond-lapping film, 3 and  $0.5 \mu\text{m}$ ), the reproducibility across the grain improves to 1.5 and 0.6‰ when the polishing relief is reduced to 15 and  $10 \mu\text{m}$ , respectively. External reproducibility in these experiments is significantly larger than 0.3‰, which we routinely obtain from well prepared flat standards with relief less than a few  $\mu\text{m}$  (Fig. 1). The possible cause of instrumental bias due to sample topography is a deformation of electrostatic field ( $-10 \text{ kV}$ ) applied to the

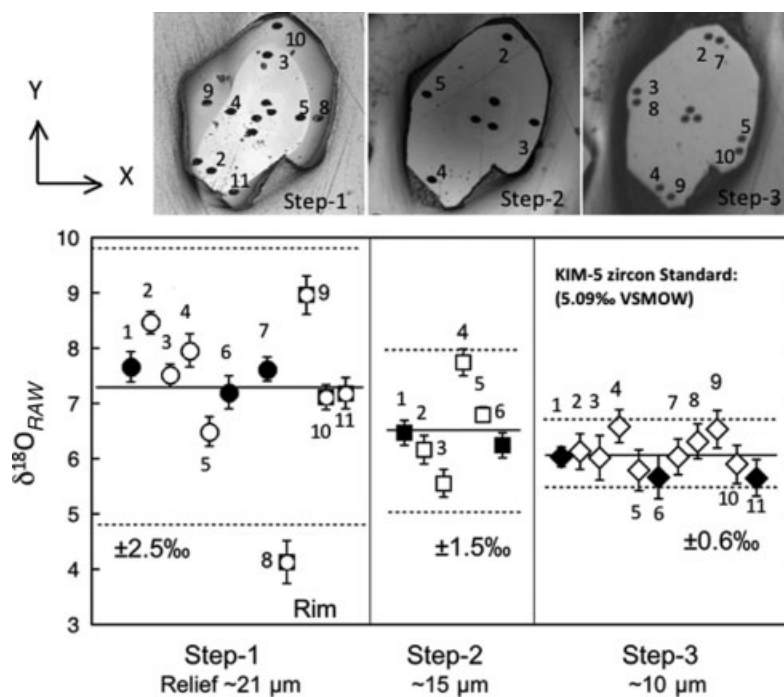


**Figure 2.** SIMS oxygen isotope analyses within a single zircon grain ( $300 \times 500 \mu\text{m}$ ) showing different levels of polishing relief.<sup>[4]</sup> A grain of zircon standard KIM-5 ( $\delta^{18}\text{O} = 5.09\text{‰}$  SMOW) was prepared with a high polishing relief by using  $0.3 \mu\text{m}$   $\text{Al}_2\text{O}_3$  powders on a fast-rotating high-nap pad ( $21 \mu\text{m}$ , Step-1). The polishing relief was subsequently ground down using a diamond lapping film for Step-2 ( $15 \mu\text{m}$ ) and Step-3 ( $10 \mu\text{m}$ ). The relief was measured using a Zygo white light profilometer. Upper images are reflected light microscope pictures of the grain at each step. The graphs below show the SIMS  $\delta^{18}\text{O}_{\text{RAW}}$  values across the grains at each step; external reproducibility is improved from  $\pm 2.5\text{‰}$  (2SD) for Step-1 to  $0.6\text{‰}$  for Step-3. Analyses of grains with less than  $2 \mu\text{m}$  of relief have precision of  $\pm 0.3\text{‰}$ . The solid and dashed lines in each test represent the average and 2SD limit of the repeated analyses.

sample surface, which displaces the trajectory of secondary ions and results in fractionation of isotopes having different mass.

The sample holder itself can also produce bias if the analysis spots are located too close to the edge of the holder. These effects are often referred to as 'X–Y effects'. In tests of such X–Y effects, zircon standard grains mounted 6–7 mm away from the center of a 25 mm epoxy mount show a small variation ( $\sim 0.4\text{‰}$ ) compared to those in the center, and the effect can be larger if the epoxy mount is not flat across the surface.<sup>[4]</sup>

## Effect of Crystal Orientation

### Oxygen isotope ratios in magnetite ( $\text{Fe}_3\text{O}_4$ )

Lyon *et al.*<sup>[10]</sup> suggested that magnetite ( $\text{Fe}_3\text{O}_4$ ) shows a crystal orientation effect of  $\pm 5\text{‰}$  for measured oxygen isotope ratios using SIMS. In this paper, 'crystal' refers to a crystalline solid without reference to crystalline faces and 'crystal orientation' (or 'crystallographic orientation') refers to the orientation of the crystal lattice relative to the instrumental geometry. We identified the same problem, but smaller in magnitude, in magnetite grains while evaluating potential SIMS standards. Multiple analyses of randomly oriented grains consistently show poor grain-to-grain reproducibility ( $\pm 2\text{‰}$ , 2SD) for seven different magnetite samples. In contrast, replicate analyses within single grains of magnetite standard are consistent within  $0.4\text{‰}$ , close to the typical reproducibility of homogeneous standard for other minerals (Fig. 3). Huberty *et al.*<sup>[11]</sup> performed Electron Back Scatter Diffraction (EBSD) analyses of these magnetite grains to measure the crystallographic orientation against direction of the Cs primary

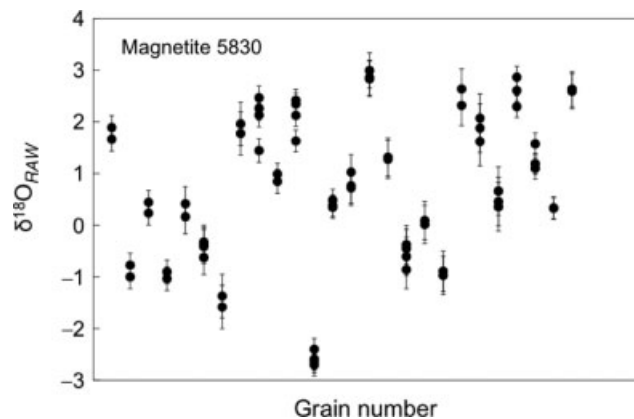


**Figure 3.** The reproducibility of oxygen isotope analyses from magnetite standard 5830 ( $\delta^{18}\text{O} = 3.95 \pm 0.31\text{‰}$  SMOW).<sup>[11]</sup> The SIMS  $\delta^{18}\text{O}_{\text{RAW}}$  values are shown for individual randomly oriented magnetite grains. The replicate analyses from each individual grain agree within the analytical uncertainty of  $\sim 0.3\text{‰}$ , while different grains differ by more than  $5\text{‰}$ .

ion beam. They found that SIMS  $\delta^{18}\text{O}_{\text{RAW}}$  values correlate with the set of directions  $\langle uv0 \rangle$ , from  $110$  to  $100$  which are preferred channeling and focusing directions for minerals with face-centered cubic crystal structures. When the incident angle of the primary ions is parallel to these directions, channeling of incident  $\text{Cs}^+$  ions and focusing of secondary ions may occur. There is also a weak correlation between the secondary ion yield and the  $\delta^{18}\text{O}_{\text{RAW}}$  values. A correlation of measured  $\delta^{18}\text{O}$  and crystal orientation has also been observed in hematite (Huberty, unpublished data), but

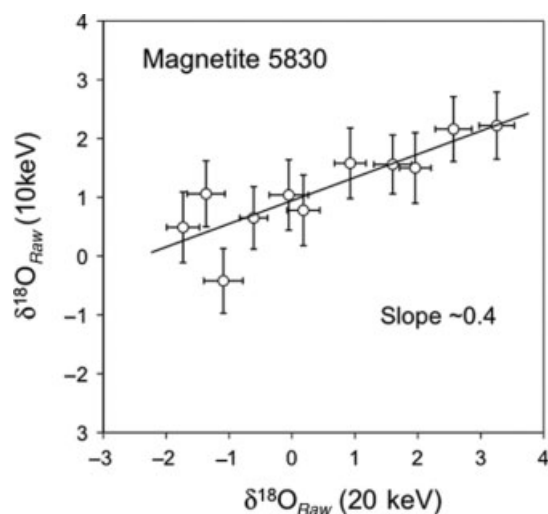


**Figure 4.** Comparison of SIMS  $\delta^{18}\text{O}_{\text{RAW}}$  values measured with different primary ion impact energies. Each data point was obtained from a single grain of magnetite standard 5830 that was placed in the same orientation, but in two different analytical conditions for  $\text{Cs}^+$  and sample acceleration voltages of +10 kV and -10 kV (X axis), and +5 kV and -5 kV (Y axis), respectively. The data correlate linearly with slope close to 0.5. The total range of variation in  $\delta^{18}\text{O}_{\text{RAW}}$  values is reduced from 5 to 2.5‰.

no measurable effect can be detected for a wide range of silicate, carbonate, or oxide minerals as shown in elsewhere.<sup>[1]</sup>

If measured isotope ratios are fractionated by ion channeling and focusing effects, the magnitude of variability should be reduced at lower impact energies of primary ions. To test this hypothesis, we conducted two sets of analyses, in which the same magnetite grains (same orientation) were analyzed with two different primary ion impact energies, by applying different primary and secondary accelerating voltages; (1) +10 kV/-10 kV (total impact energy of 20 keV) and (2) +5 kV/-5 kV (total impact energy of 10 keV). In these two conditions, the incident angle of  $\text{Cs}^+$  ions against the normal to the sample surface stays constant ( $\sim 21^\circ$ ). The  $\delta^{18}\text{O}_{\text{RAW}}$  values of multiple grains of magnetite standard are compared in Fig. 4, showing that the total range of  $\delta^{18}\text{O}_{\text{RAW}}$  values reduced from 5 to 2.5‰ as the primary ion impact energy is reduced from 20 to 10 keV. This suggests that the reduction in impact energy improves the analytical reproducibility, and thus, the accuracy of  $\delta^{18}\text{O}$  analyses.

### Iron isotope ratios in magnetite ( $\text{Fe}_3\text{O}_4$ )

Iron isotope analyses ( $^{56}\text{Fe}/^{54}\text{Fe}$ ) were performed on magnetite from a Banded Iron Formation sample (Biwabik Iron Formation, Minnesota) to evaluate possible crystal orientation effects. This magnetite sample was chosen due to Fe isotope homogeneity ( $\pm 0.07\text{‰}$  in 2SD for  $^{56}\text{Fe}/^{54}\text{Fe}$ ) analyzed from 12 grains that weighed between 0.17 and 0.80 mg using conventional high-precision Multi-collector Inductively Coupled Plasma Mass Spectrometry (MC-ICPMS).<sup>[12]</sup> By IMS-1280, we used  $\text{O}^-$  primary ions (-13 kV, Duoplasmatron source) in Köhler illumination mode with a 25  $\mu\text{m}$  diameter beam and primary ion intensity of 7 nA. The secondary  $\text{Fe}^+$  ions are accelerated by +10 kV. The setting of transfer lens optics is similar to that for oxygen isotopes. The entrance slit, field aperture, energy slit, and exit slits are set to 120  $\mu\text{m}$ , 6000  $\times$  6000  $\mu\text{m}$  square, 40 eV for low energy ions, and 400  $\mu\text{m}$ , respectively. We used 'X-Y mode' for secondary optics that minimizes field aberration in the mass spectrum by using a set

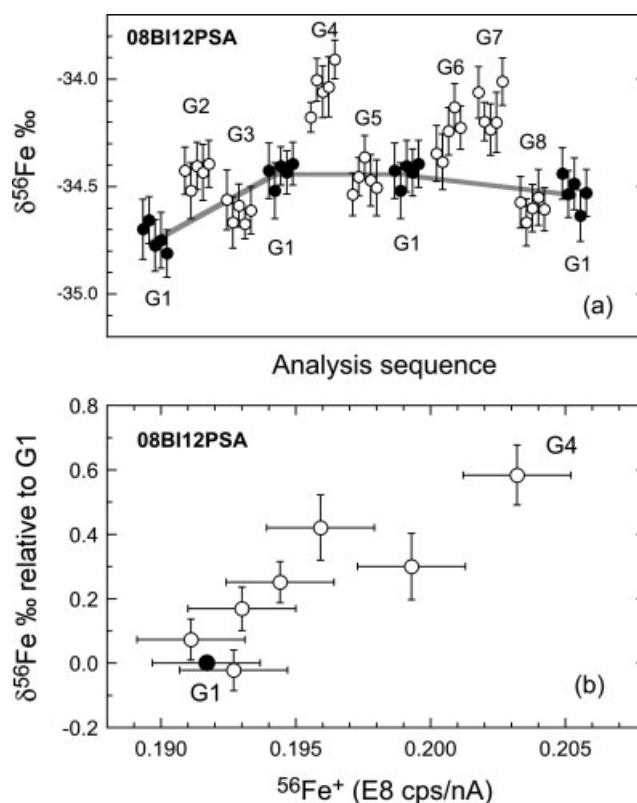


**Figure 5.** Measured  $^{56}\text{Fe}/^{54}\text{Fe}$  ratios of magnetite sample 08BI12 reported as  $\delta^{56}\text{Fe}$  values (‰ deviations from bulk earth,  $^{56}\text{Fe}/^{54}\text{Fe} = 15.70278$ ).<sup>[13]</sup> (a) Plot of measured  $\delta^{56}\text{Fe}$  values for individual spot analyses versus analysis sequence. Error bars are 2 standard errors (typically 0.15‰). Grain 1 (G1, filled symbols) was repeatedly analyzed during the analysis of seven other grains (G2–G8, open symbols) over the  $\sim 4.5$  h analytical session. External reproducibility based on the 2SD of multiple spot analyses of each magnetite grain is typically 0.2‰ in  $^{56}\text{Fe}/^{54}\text{Fe}$ . (b) Average  $\delta^{56}\text{Fe}$  values of magnetite grains relative to running standard G1 versus secondary ion yield (shown as secondary  $^{56}\text{Fe}^+$  ion intensity per primary ion intensity).

of two rectangular lenses. The isotopes of  $^{54}\text{Fe}^+$  and  $^{56}\text{Fe}^+$  were detected using two multicollection FC detectors. The secondary ion intensity of  $^{56}\text{Fe}^+$  was typically  $1.5 \times 10^8$  cps. Mass resolving power was 2200 (at 10% peak height). In addition to Fe isotopes, the  $^{53}\text{Cr}^+$  signal was monitored using a multicollector EM, which was consistently at a very low level, thus the  $^{54}\text{Cr}$  correction was insignificant. A single analysis takes 4 min, including presputtering (60 s), automatic centering (90 s), and the integration of Fe isotope signals (total 80 s; 4 s  $\times$  20 cycles). Both internal and external precisions for a single grain are 0.1–0.2‰ for ( $^{56}\text{Fe}/^{54}\text{Fe}$ ) ratios.

Measurements on multiple grains of magnetite samples, which are isotopically homogeneous, show grain-to-grain heterogeneity of 0.6‰ in  $\delta^{56}\text{Fe}$  (Fig. 5(a)). There is a positive correlation between  $^{56}\text{Fe}^+$  ion yield and  $\delta^{56}\text{Fe}$  values (Fig. 5(b)). We note that magnetite is homogenous in major element composition, with an average  $\text{Fe}_3\text{O}_4$  wt% of  $99.27 \pm 0.26\%$  (2SD) ( $N = 50$  from electron microprobe analyses), indicating that ion yield variation at the level of 10% is not a result of Fe concentration. Rather, the measured Fe isotope variability may be a result of an instrumental bias that changes with magnetite crystal orientation. Ion channeling may result in higher abundance of implanted oxygen in the mineral structure, and enhance secondary ion yield because ionization efficiency of  $\text{Fe}^+$  is higher under more oxidized conditions, such as using  $\text{O}_2^-$  primary ions. If this hypothesis is correct, instru-

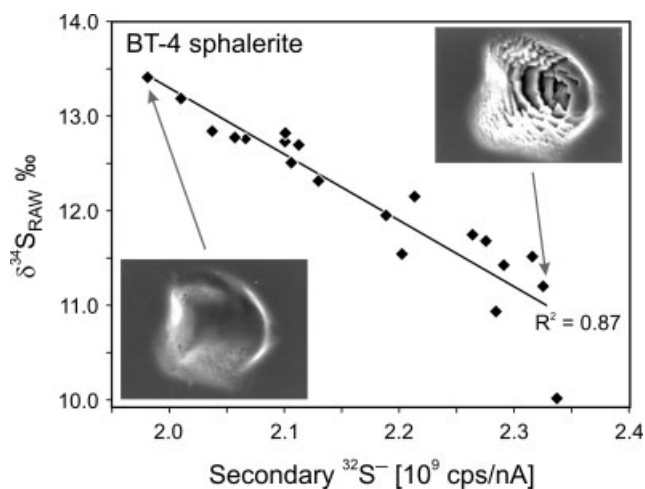


**Figure 6.** The crystal orientation effect on sulfur isotope ratios ( $^{34}\text{S}/^{32}\text{S}$ ) in sphalerite (ZnS) standard (BT-4). Data are from Ref. [14]. The measured values are normalized to the ( $^{34}\text{S}/^{32}\text{S}$ ) ratio of V-CDT ( $^{34}\text{S}/^{32}\text{S} = 1/22.6436^{[15]}$ ) and shown as delta notation. Each individual data point is from a different randomly oriented grain. While each grain is homogeneous, there is a strong negative correlation of  $\delta^{34}\text{S}_{\text{RAW}}$  with secondary  $^{32}\text{S}^-$  ion yield from grain-to-grain (shown as secondary  $^{32}\text{S}^-$  ion intensity per primary ion intensity). Inserted SEM images after SIMS analyses are from two grains with higher and lower  $\delta^{34}\text{S}_{\text{RAW}}$  values, showing smooth and rough SIMS crater morphologies, respectively. Other pits show intermediate textures. The EBSD analyses indicate that the crystal orientation of a grain with smooth crater morphologies is such that the primary Cs beam was nearly parallel to 110. Thus, ion channeling reduces secondary ion yield and enriches  $^{34}\text{S}^-$ .

mental fractionation of Fe isotope favors the heavy isotope in ion channeling conditions, as is the case for oxygen isotopes.

### Sulfur isotope ratios in sphalerite (ZnS)

Sulfur isotope ratio ( $^{34}\text{S}/^{32}\text{S}$ ) analysis in sulfide minerals is performed using an IMS-1280 at WiscSIMS with conditions similar to those of oxygen two-isotope analyses. Kozdon *et al.*<sup>[14]</sup> reported a crystal orientation effect on the SIMS  $\delta^{34}\text{S}_{\text{RAW}}$  values from the analyses of sphalerite (ZnS) standard grains. Similar to the case of oxygen isotope analyses of magnetite,  $\delta^{34}\text{S}_{\text{RAW}}$  values of sphalerite are reproducible at  $\pm 0.3\text{‰}$  within a single grain, while significant variations of  $\delta^{34}\text{S}_{\text{RAW}}$  values are observed among multiple randomly oriented sphalerite grains. There is a strong negative correlation between secondary  $\text{S}^-$  ion yield and  $\delta^{34}\text{S}$  values (Fig. 6). The ionization yield changes by nearly 20% and is associated with the morphology of SIMS pit bottoms that change from a smooth surface at low ion yields to a significantly rough surface at high ion yields (Fig. 6). EBSD analyses of these grains show that grains with low ionization yield and high  $\delta^{34}\text{S}_{\text{RAW}}$  values are measured when the direction of the  $\text{Cs}^+$  beam is parallel to  $\langle u\bar{u}w \rangle$ , from 111 to 110, which are the preferred channeling and focusing directions in minerals with diamond-cubic crystal structures like sphalerite. Preliminary results also show an orientation effect for measurements of  $^{34}\text{S}/^{32}\text{S}$  in galena, but no measureable effect for pyrite, chalcopyrite or pyrrhotite (Kozdon, unpublished data).

## Conclusion

We have demonstrated that the IMS-1280 is capable of obtaining high precision ( $\leq 0.3\text{‰}$ ) analyses of oxygen, sulfur, and iron isotope ratios from geological samples at the  $10\ \mu\text{m}$  scale. We also recognized analytical artifacts in the IMS-1280 data at the level of a few permil or more related to sample topography and crystal orientation effects. In addition to magnetite and sphalerite, hematite ( $\text{Fe}_2\text{O}_3$ ) and galena ( $\text{PbS}$ ) seem to show similar crystal orientation effects. However, it should be emphasized that the crystal orientation effect has not been identified from numerous other minerals that have been evaluated as standards for oxygen and sulfur isotope analyses,<sup>[1,14]</sup> even though some of these mineral structures are similar to those of magnetite and sphalerite. Therefore, the exact mechanism of isotopic fractionation due to crystal orientation, and the role of channeling and focusing are not yet fully understood. The sample topography and X–Y effects can be avoided by the careful sample preparation and subsequent evaluation of polishing relief, which should be in the order of a few  $\mu\text{m}$  or less for individual samples. Crystal orientation effect is reduced by decreasing the primary ion sputtering energy.

## Acknowledgements

The WiscSIMS laboratory is partly supported by NSF (EAR03-19230, EAR07-44079). Parts of this research were supported by the NASA Astrobiology Institute, NASA (NNA08CN86A) and DOE (93ER14389). We thank J. Kern and B. Hess for technical support and sample preparation.

## References

- [1] J. W. Valley, N. T. Kita, *Mineralogical Association of Canada Short Course* **2009**, 41, 19.
- [2] I. J. Orland, M. Bar-Matthews, N. T. Kita, A. Ayalon, A. Matthews, J. W. Valley, *Quaternary Research* **2009**, 71, 27.
- [3] R. Kozdon, T. Ushikubo, N. T. Kita, M. J. Spicuzza, J. W. Valley, *Chem. Geol.* **2009**, 258, 327.
- [4] N. T. Kita, T. Ushikubo, B. Fu, J. W. Valley, *Chem. Geol.* **2009**, 264, 43.
- [5] P. Baertschi, *Earth Planet. Sci. Lett.* **1976**, 31, 341.
- [6] J. W. Valley, N. E. Kitchen, M. J. Kohn, C. R. Niendorf, M. J. Spicuzza, *Geochim. Cosmochim. Acta* **1995**, 59, 5223.
- [7] F. Z. Page, T. Ushikubo, N. T. Kita, L. R. Riciputi, J. W. Valley, *Am. Mineral.* **2007**, 92, 1772.
- [8] T. Nakamura, T. Noguchi, A. Tsuchiyama, T. Ushikubo, N. T. Kita, J. W. Valley, M. E. Zolensky, Y. Kakazu, K. Sakamoto, E. Mashio, K. Uesugi, T. Nakano, *Science* **2008**, 321, 1664.
- [9] G. Slodzian, F. Hillion, F. J. Stadermann, E. Zinner, *Appl. Surf. Sci.* **2004**, 231–232, 874.
- [10] I. C. Lyon, J. M. Saxton, S. J. Cornah, *Int. J. Mass Spectrom. Ion Proc.* **1998**, 172, 115.
- [11] J. M. Huberty, N. T. Kita, P. R. Heck, R. Kozdon, J. H. Fournelle, H. F. Xu, J. W. Valley, *Geochim. Cosmochim. Acta Suppl.* **2009**, 73, A562.
- [12] B. L. Beard, C. M. Johnson, J. L. Skulan, K. H. Nealson, L. Cox, H. Sun, *Chem. Geol.* **2003**, 195, 87.
- [13] B. L. Beard, C. M. Johnson, *Geochim. Cosmochim. Acta* **1999**, 63, 1653.
- [14] R. Kozdon, N. T. Kita, J. A. Huberty, J. H. Fournelle, J. W. Valley, *Eos Trans. AGU* **2009**, 90(52), Fall Meet. Suppl., Abstract V31E-2019.
- [15] T. Ding, S. Valkiers, H. Kipphardt, P. De Bièvre, P. D. P. Taylor, R. Gonfiantini, R. Krouse, *Geochim. Cosmochim. Acta* **2001**, 65, 2433.